Supporting Information

Multicolor circularly polarized luminescence inversion of metal-organic supramolecular polymers

Kuo Fu, Guofeng Liu*

School of Chemical Science and Engineering, Advanced Research Institute, Tongji University, Shanghai, 200092, P. R. China.

E-mail: liuguofeng@tongji.edu.cn

1 Experimental section

Instruments and methods.

NMR spectra were recorded on a Bruker AVANCE III HD 400 MHz and 600 MHz Instrument at ambient temperature. Circular dichroism (CD) spectra were obtained using JASCO J-810 CD spectrometer with a bandwidth of 1.0 nm, scanning speed of 500 nm min^{-1}, and data integration time of 1 s. CD spectra of gels were recorded in the UV/Vis region (250–800 nm) using a 0.1 mm quartz cuvette with the gelator concentration at 14 mM. Scanning electron microscopy (SEM) was performed on a JSM-7900F with an accelerating voltage of 3 kV. Before SEM measurements, the samples of depositing dilute solutions of gels on silicon wafers were coated with a thin layer of Pt to increase the contrast. Mass spectral data were obtained by using a SolariX maldi-FTMS instrument. Fourier transforms infrared (FT-IR) spectra were recorded using Thermo Scientific Nicolet iS10. CPL measurements were performed with JASCO CPL-300 spectrometer, the Ex and Em slit width of 3000 μm, scanning speed of 500 nm min^{-1}, and data integration time of 1 s. CPL spectra of gels were measured using a 0.1 mm quartz cuvette with the gelator concentration at 14 mM. Fluorescence spectra were obtained using an F-4500 fluorescence spectrophotometer. The rheology of the gels was measured with EC TWIST30 from Anton Paar. We used a 25 mm parallel plate geometry with a sand-blasted surface to prevent slip. After placing the sample, the upper plate was slowly lowered until a gap of size 0.3 mm was reached. Excess gel was trimmed just before the final gap height was reached. At that point, we performed first the frequency sweep, then the strain sweep, and finally the recovery test. The Peltier plate kept the samples at a constant temperature of 25℃. The oscilatory strain sweep measurements were performed at a frequency of 1 Hz, while the frequency sweeps were performed at a constant strain amplitude of 0.01%.

Material.

5-bromothiophene-2-carbaldehyde, 4-hydroxyphenylboronic acid, potassium carbonate, 4-pyridylacetonitrile, tetrakis(triphenylphosphine)palladium, triethylamine, pyrrolidine, cholesteryl chloroformate, aluminum chloride, cobalt chloride, copper chloride, zinc chloride, bismuth chloride, ferrous chloride and ferric chloride were purchased from Shanghai Titan Scientific Co., Ltd. Silver nitrate was purchased from Sinopharm Chemical Reagent Co., Ltd. The organic solvents were purchased from Shanghai Titan Scientific Co., Ltd. without further purification.

Metallogel preparation.

Ultrasound: A typical protocol for fabricating metallogels in organic solvents involves the following steps: the stock solution of metal ions was added into PCSPCC molecular with a concentration of 14 mM (n_{PCSPCC}/n_{M}^{n+} = 2/1). The mixture was sonicated for 1 minute, followed by several minutes of rest at room temperature, resulting in the formation of metallogels.

Heating-cooling cycle: A typical protocol for fabricating metallogels in organic solvents involves the following steps: the stock solution of metal ions was added into PCSPCC molecular with a concentration of 14 mM (n_{PCSPCC}/n_{M}^{n+} = 2/1). The mixture was sonicated for 1 minute, followed by the mixture being heated at 373 K for 1 min, and rested for several minutes at room temperature, resulting in the formation of metallogels.

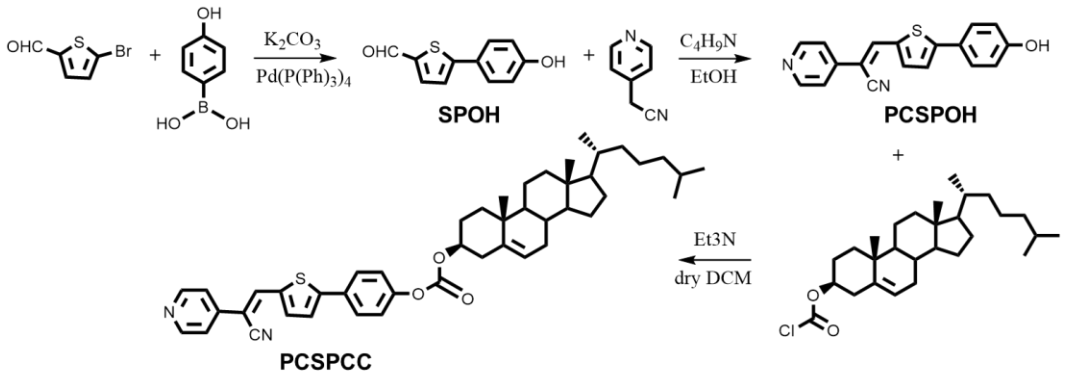

Scheme S1 Synthetic route of PCSPCC.

Synthesis of SPOH. 5-bromothiophene-2-carbaldehyde (1 g, 5.26 mmol), 4-hydroxyphenylboronic acid (1.08 g, 7.89 mmol), and tetrakis(triphenylphosphine) palladium (0.304 g, 0.263 mmol) were added to the flask with two necks. Under the N_2 atmosphere, the 60 mL THF and the 12 mL potassium carbonate aqueous solution (7.23g, 52.6 mmol) were added. Then the whole system was refluxed at 75 °C for 12 h. After that, the whole system was cooled to room temperature, and then extracted three times with EA/H_2O, and the solid residue was purified by column chromatography (silica gel: DCM/EA, 10/1, *v*/*v*) to give 0.73 g yellow powder (yield: 68%). ^{1}H NMR (600 MHz, DMSO-d_6) δ 10.01 (s, 1H), 9.86 (s, 1H), 7.99 (d, *J* = 3.9 Hz, 1H), 7.64 (d, *J* = 8.4 Hz, 2H), 7.56 (d, *J* = 4.0 Hz, 1H), 6.86 (d, *J* = 8.4 Hz, 2H). ^{13}C NMR (151 MHz,

DMSO-d_6) δ 184.13, 159.48, 154.19, 140.91, 140.05, 128.33, 123.98, 123.86, 116.57.

Synthesis of PCSPOH. SPOH (0.5 g, 2.45 mmol) and 4-nitrobenzyl cyanide (0.32 g, 2.70 mmol) were dissolved into 50 mL of ethanol, which was stirred at 80 °C to form a uniform solution. After that, pyrrolidine (0.1 mL) was added to the above solution and the reaction was continued for 12 h. A large number of yellow solids precipitated during the cooling process of the reaction system, and the yellow solids were separated from the reaction solution by vacuum filtration, which was further purified via repeated washing with ethanol to produce pure PCSPOH as a yellow solid (0.62 g, yield: 83%). ^{1}H NMR (600 MHz, DMSO-d_6) δ 9.98 (s, 1H), 8.66 (d, J = 6.1 Hz, 2H), 8.55 (s, 1H), 7.80 (d, J = 4.0 Hz, 1H), 7.68 (d, J = 6.2 Hz, 2H), 7.62 (d, J = 8.6 Hz, 2H), 7.56 (d, J = 3.9 Hz, 1H), 6.88 (d, J = 8.6 Hz, 2H). ^{13}C NMR (151 MHz, DMSO) δ 159.27, 151.53, 150.90, 141.50, 139.15, 139.08, 135.05, 128.10, 124.11, 123.47, 119.74, 117.93, 116.67, 102.40, 40.41, 40.27, 40.13, 39.99, 39.85, 39.71, 39.57, 0.58.

Synthesis of PCSPCC. PCSPOH (0.5 g, 1.64 mmol) was dispersed by 10 mL dry dichloromethane containing Et_3N (0.2 mL), and the mixed solution was added dropwise to 50 mL dichloromethane solution containing Et_3N (0.24 mL, 1.68 mmol) and cholesteryl chloroformate (0.81 g, 1.80 mmol) in the ice bath and stirring 10 min. After stirring at room temperature for 3 h and evaporating under vacuum, the crude product was purified by column chromatography on silica gel (ethyl acetate/dichloromethane, 1/10) to give PCSPCC in 82 % yield. ^{1}H NMR (400 MHz, Chloroform-d) δ 8.67 (d, J = 6.2 Hz, 2H), 7.82 (s, 1H), 7.73 – 7.63 (m, 3H), 7.54 (d, J = 6.4 Hz, 2H), 7.35 (d, J = 4.0 Hz, 1H), 7.27 (d, J = 8.6 Hz, 2H), 5.43 (d, J = 5.1 Hz, 1H), 4.60 (tt, J = 10.7, 5.2 Hz, 1H), 2.49 (t, J = 7.5 Hz, 2H), 2.09 – 1.90 (m, 4H), 1.86 – 1.68 (m, 2H), 1.62 – 1.44 (m, 6H), 1.39 – 1.23 (m, 4H), 1.22 – 0.97 (m, 13H), 0.92 (d, J = 6.5 Hz, 3H), 0.86 (dd, J = 6.6, 1.9 Hz, 6H), 0.68 (s, 3H). ^{13}C NMR (151 MHz, Chloroform-d) δ 152.63, 151.68, 150.26, 139.04, 136.93, 136.19, 127.44, 124.19, 123.32, 121.92, 119.57, 79.19, 56.67, 56.12, 49.97, 42.31, 39.70, 39.51, 37.93, 36.82, 36.55, 36.17, 35.79, 31.91, 31.83, 28.23, 28.02, 27.64, 24.28, 23.82, 22.83, 22.57, 21.05, 19.29, 18.72, 11.87. EI-MS (m/z) for $C_{46}H_{56}N_2O_3S$ calcd. 716.401; found 717.375 $[M + H]^+$.

2 Additional experimental data and figures

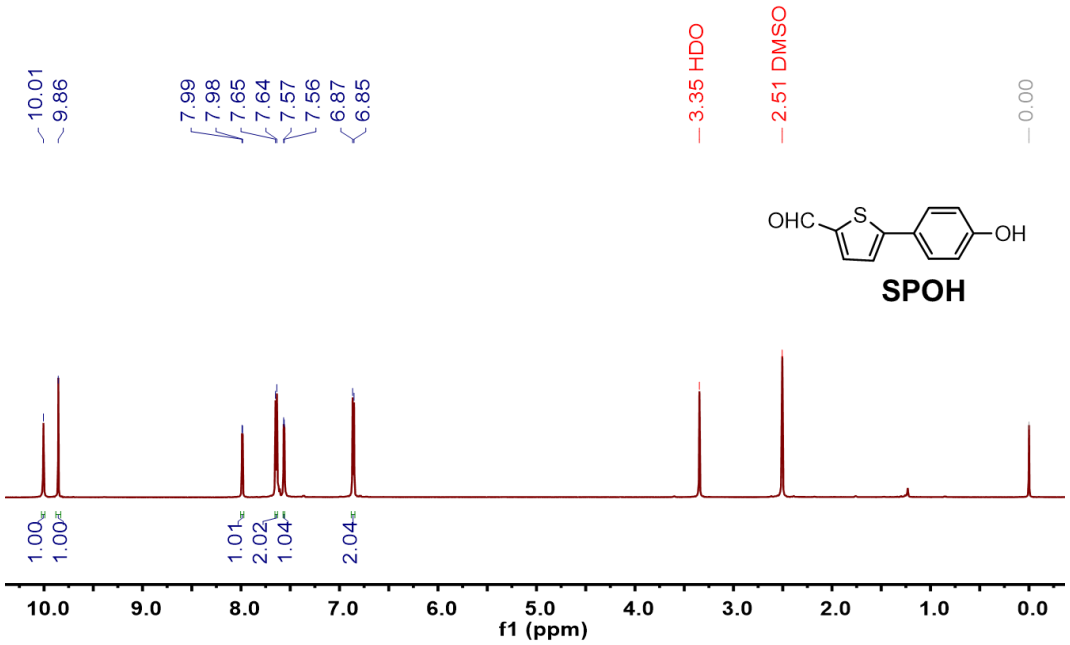

Figure S1. ^{1}H NMR spectrum of **SPOH** in DMSO-d_6.

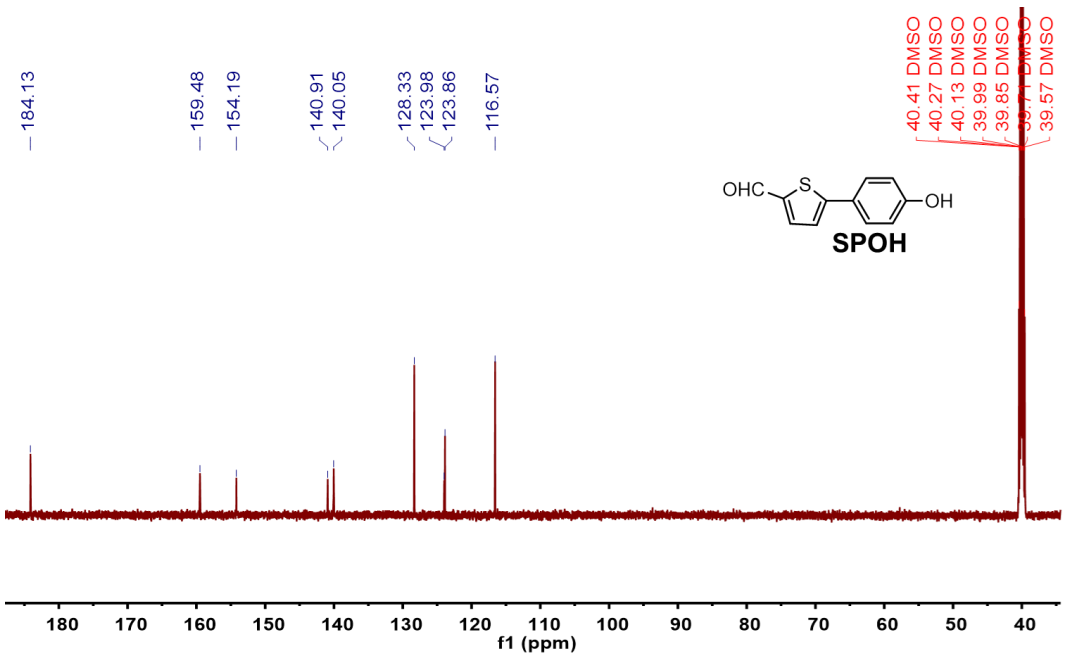

Figure S2. ^{13}C NMR spectrum of **SPOH** in DMSO-d_6.

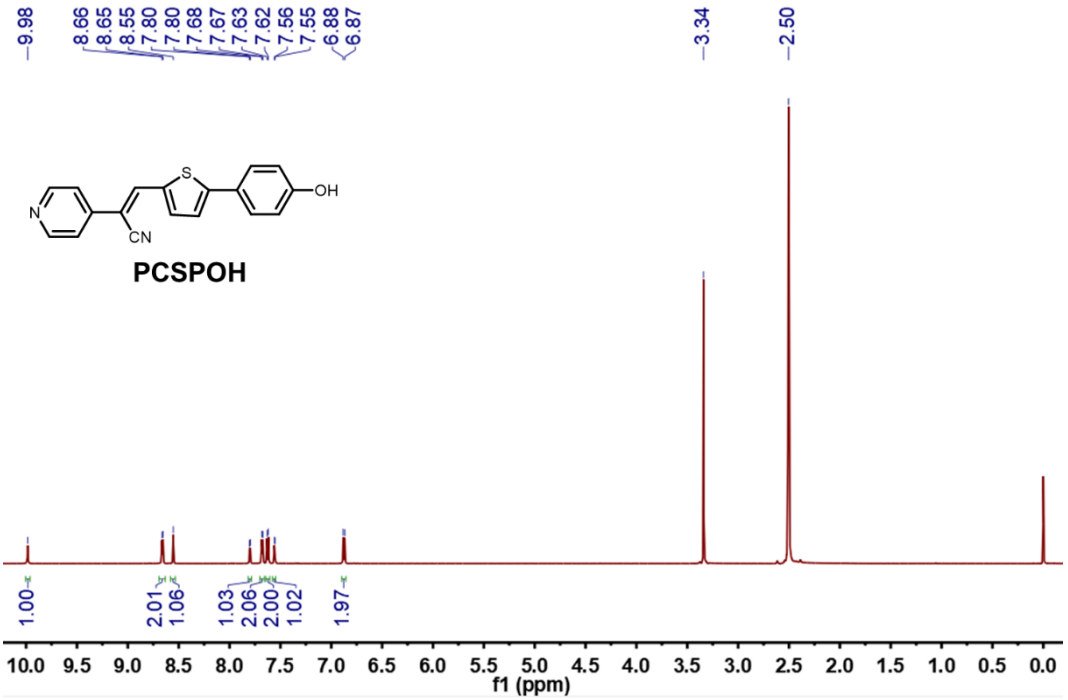

Figure S3. ^{1}H NMR spectrum of **PCSPOH** in DMSO-d_6.

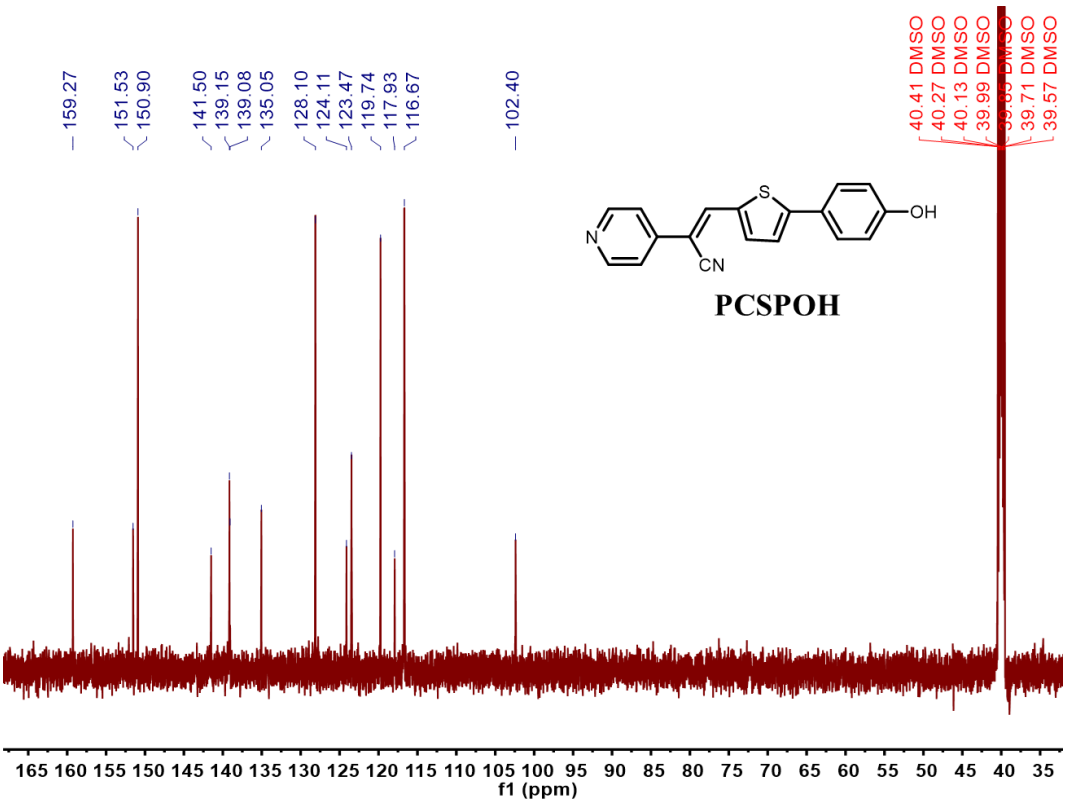

Figure S4. ^{13}C NMR spectrum of **PCSPOH** in DMSO-d_6.

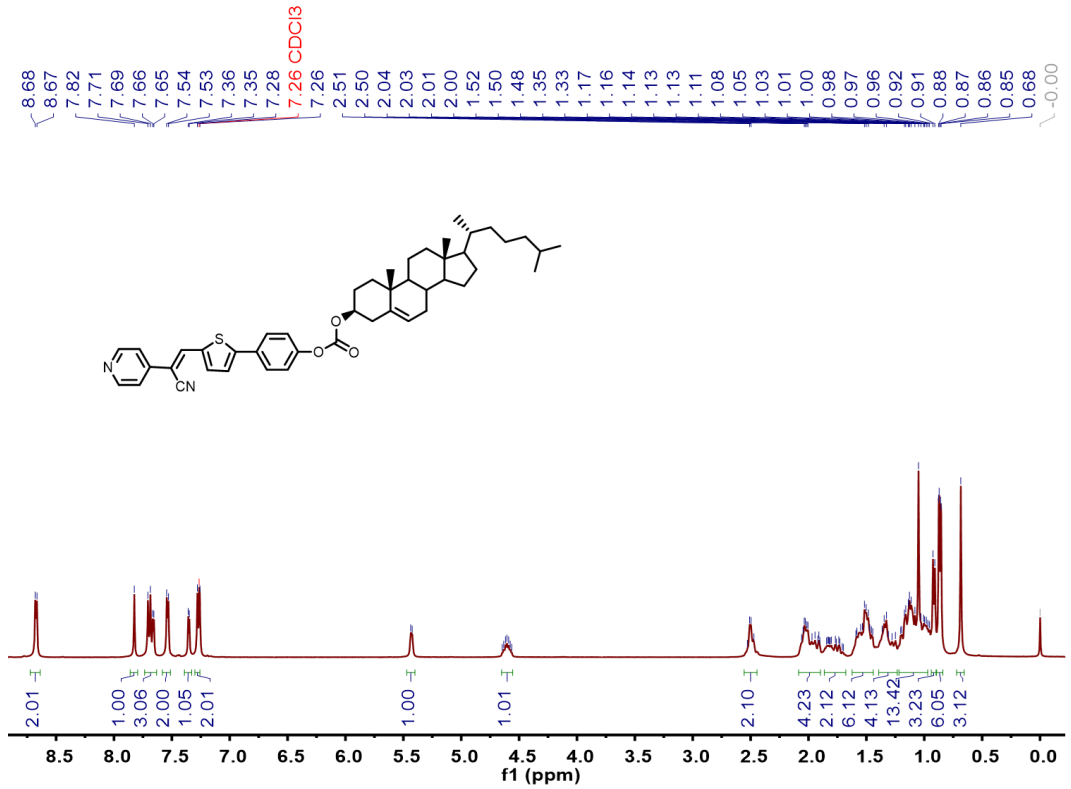

Figure S5. ^{1}H NMR spectrum of **PCSPCC** in $CDCl_3$.

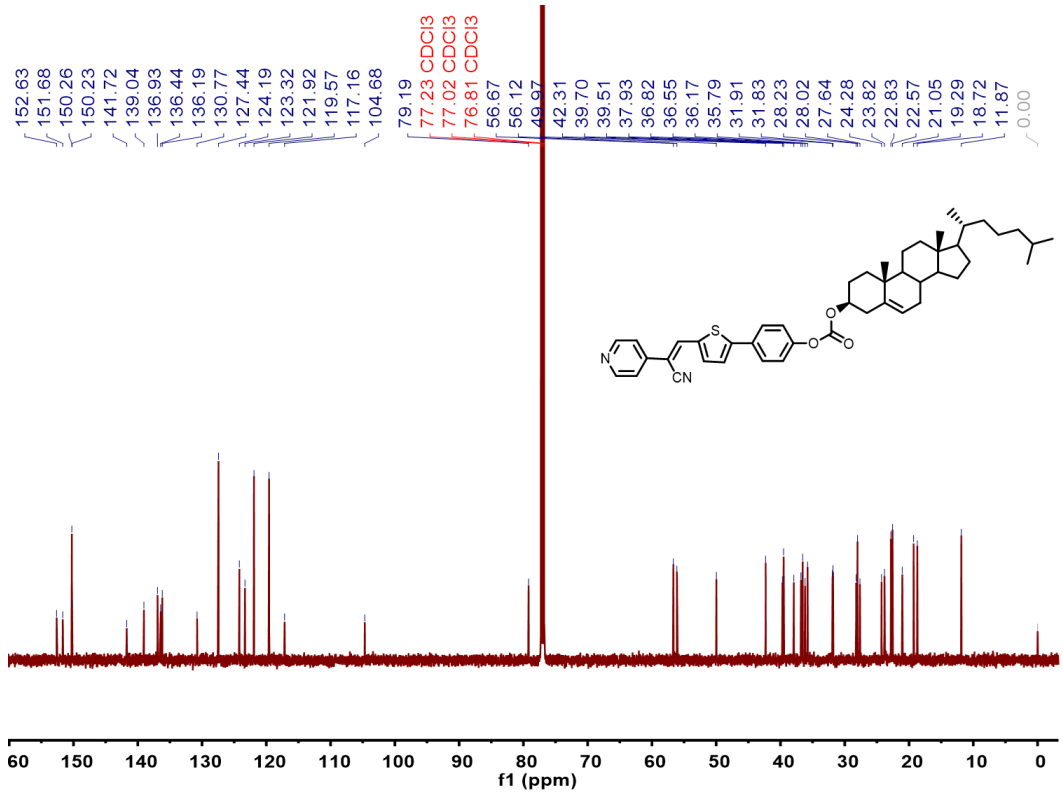

Figure S6. ^{13}C NMR spectrum of **PCSPCC** in $CDCl_3$.

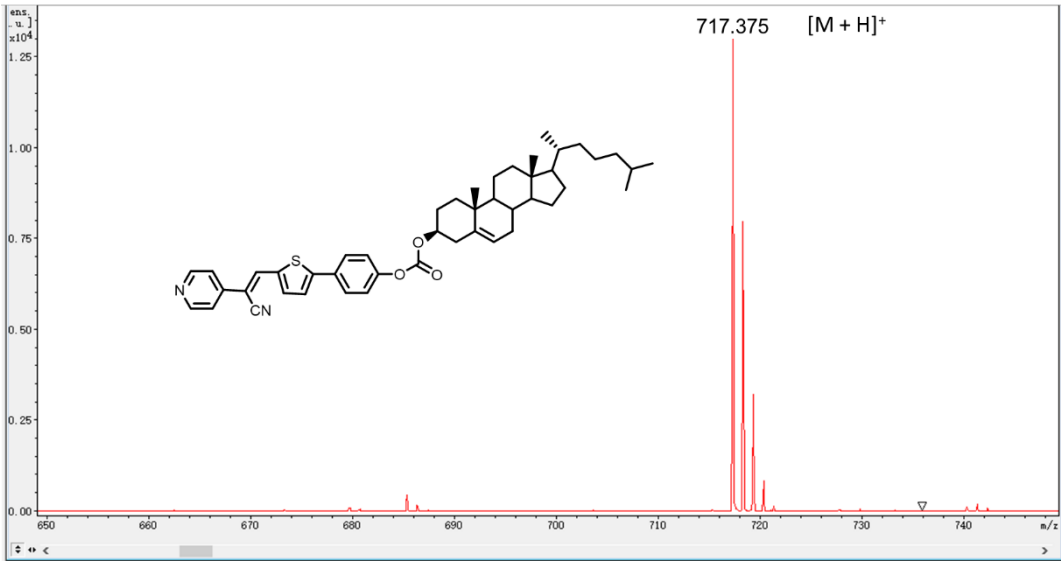

Figure S7. HRMS spectrum of PCSPCC.

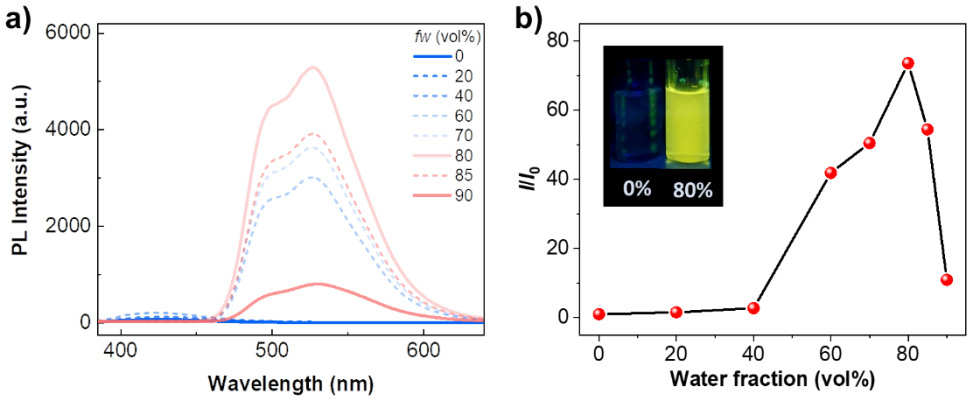

Figure S8. a) The photoluminescence spectra of PCSPCC in THF/H_2O mixtures with different water fractions (f_w, vol%). The excitation wavelength was 365 nm. b) The relative PL intensity of PCSPCC with different f_w. I_0 is the PL intensity of PCSPCC at 527 nm in pure THF. Insets are the images of PCSPCC with 0% and 80% water fraction under the irradiation of 365 nm UV lamp.

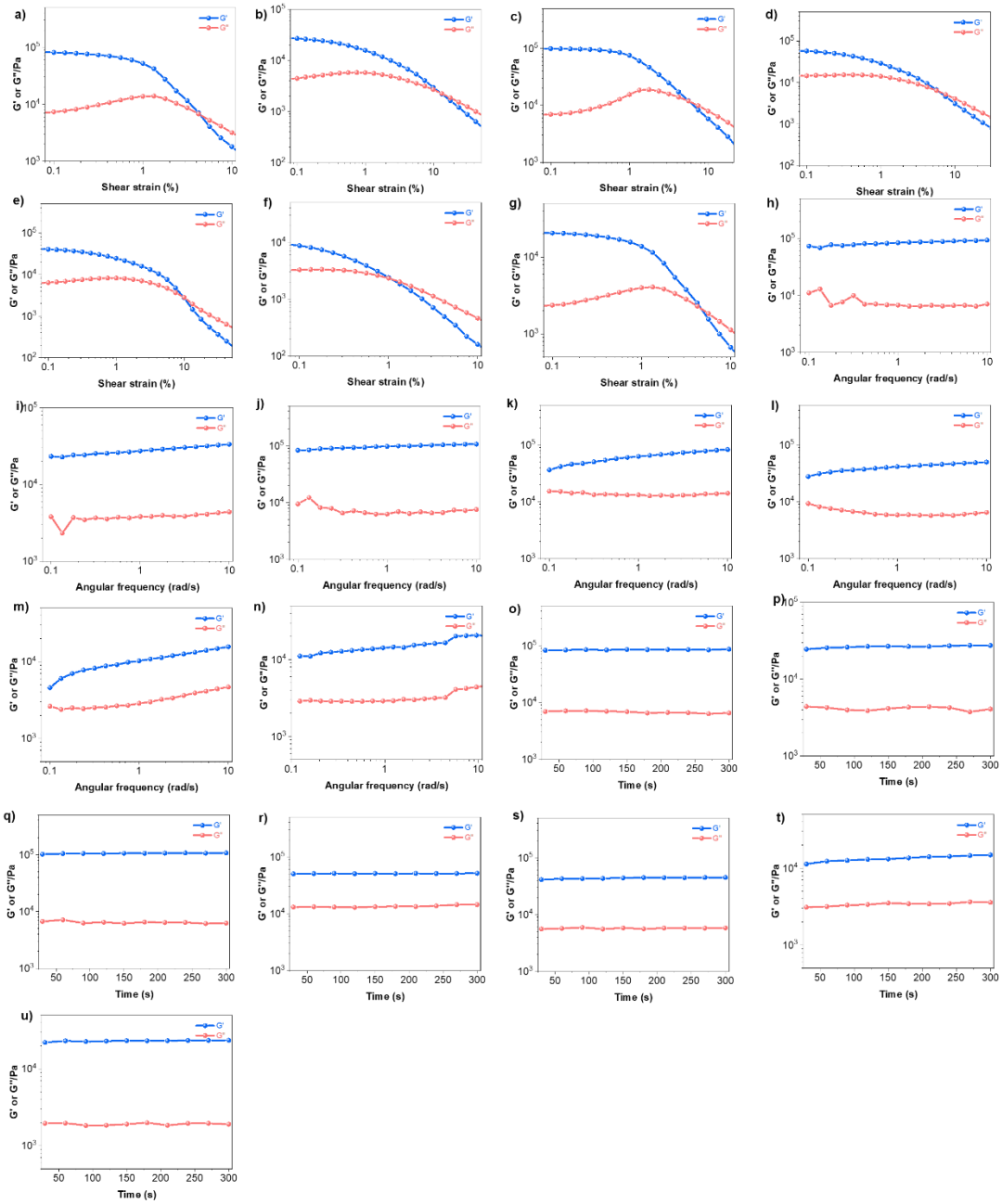

Figure S9. The dynamic strain sweep of PCSPCC in a) DMF, b) EtOH, c) DMSO,d) EA, e) Dio, f) PX, g) n-BuOH at a constant frequency of 1 rad/s over a strain range of 0.01−50%. Plots of frequency-dependent rheological measurements of PCSPCC in h) DMF, i) EtOH, j) DMSO, k) EA, l) Dio, m) PX, n) n-BuOH with a shear strain of 0.01% at 25 °C.Rheological analysis of recovery tests of PCSPCC in o) DMF, p) EtOH, q) DMSO, r) EA, s) Dio,t) PX, u) n-BuOH at a constant frequency of 1 rad/s and with a shear strain of 0.01% at 25 °C.

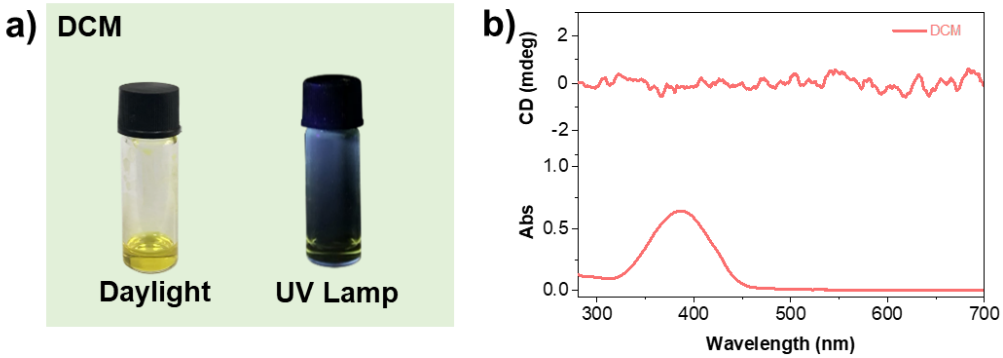

Figure S10. a) The photograph of PCSPCC in DCM under the irradiation of daylight and UV light. b) CD spectrum of PCSPCC in DCM. The concentration of PCSPCC was fixed at 14 mM.

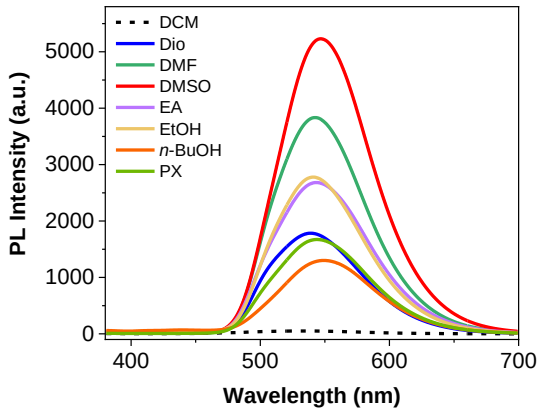

Figure S11. The photoluminescence spectra of PCSPCC ([PCSPCC] = 14 mM) obtained from various solvents.

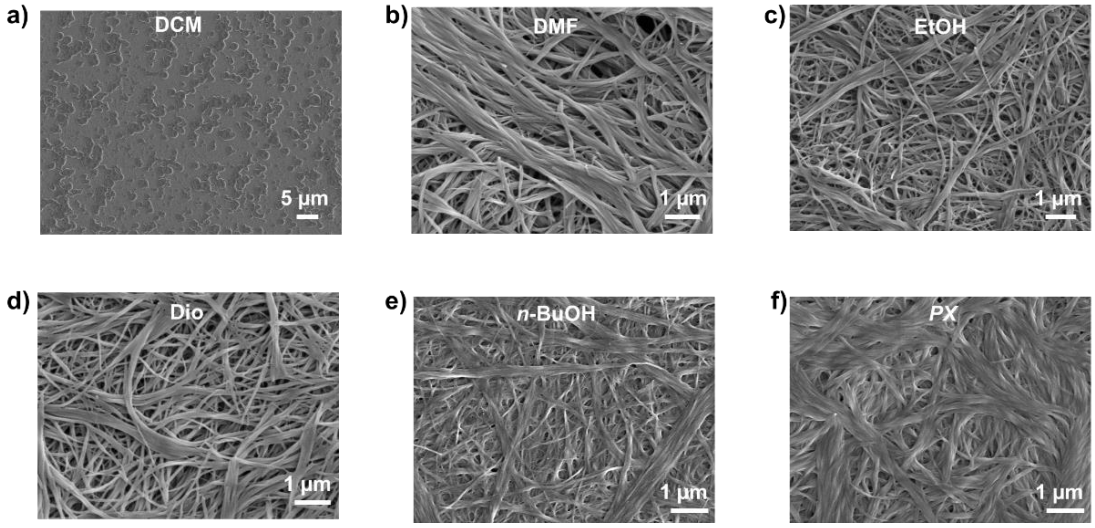

Figure S12. SEM image of PCSPCC aggregates obtained from a) DCM, b) DMF, c) EtOH, d) Dio, e) *n*-BuOH, and f) PX. The concentration of PCSPCC was fixed at 14 mM.

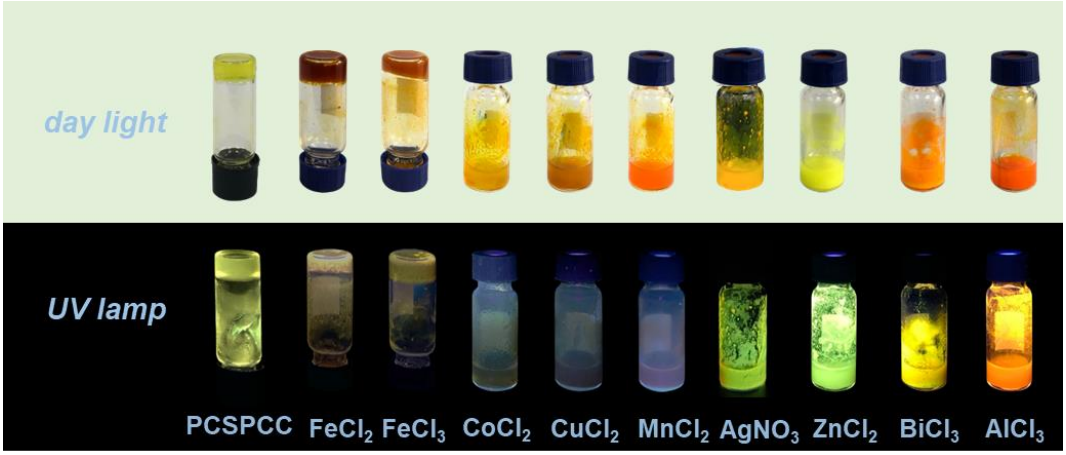

Figure S13. The photographs of PCSPCC-based MOSPs formed in *n*-BuOH under the irradiation of daylight and UV light ([PCSPCC] = 14 mM, $n_{M^{n+}}/n_{PCSPCC}$ = 1/2).

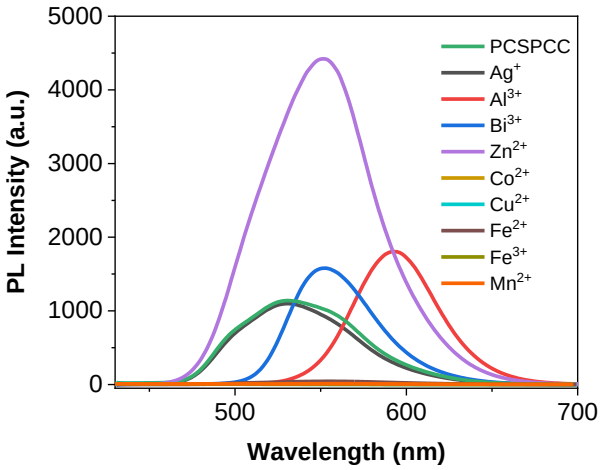

Figure S14. The photoluminescence spectra of PCSPCC-based MOSPs in *n*-BuOH ([PCSPCC] = 14 mM, $n_{M^{n+}}/n_{PCSPCC}$ = 1/2).

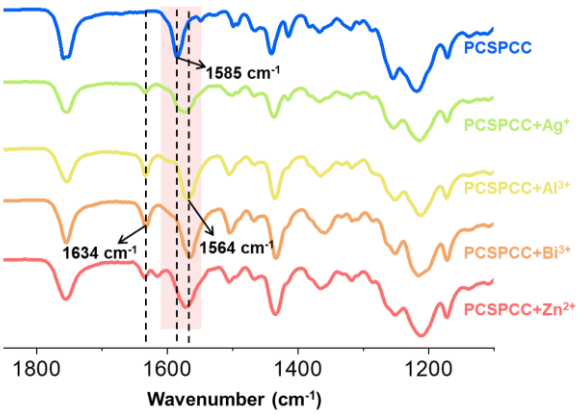

Figure S15. FT-IR spectra of PCSPCC powder and the aggregates of PCSPCC+$AgNO_3$, PCSPCC+$AlCl_3$, PCSPCC+$BiCl_3$, and PCSPCC+$ZnCl_2$ treated by heating-cooling cycle. The band of ~1585 cm^{-1} was assigned to the characteristic peaks of pyridyl moiety, while the stretching vibration band was shifted to ~1564 cm^{-1} and a new band was observed around 1634 cm^{-1} after adding metal ions, confirming strong coordination of the nitrogen atom from the aromatic ring (pyridyl) with the metal ions.[1-4]

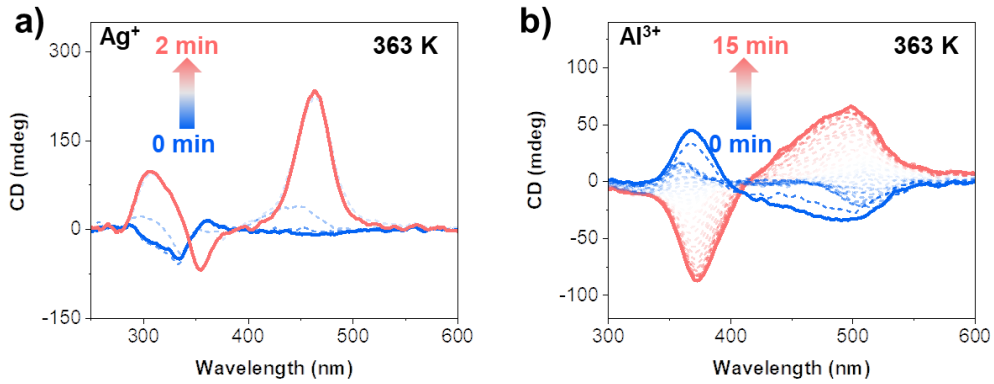

Figure S16. Time-dependent CD spectra of a) PCSPCC+Ag^+ and b) PCSPCC+Al^{3+} aggregates in a cuvette at 363 K.

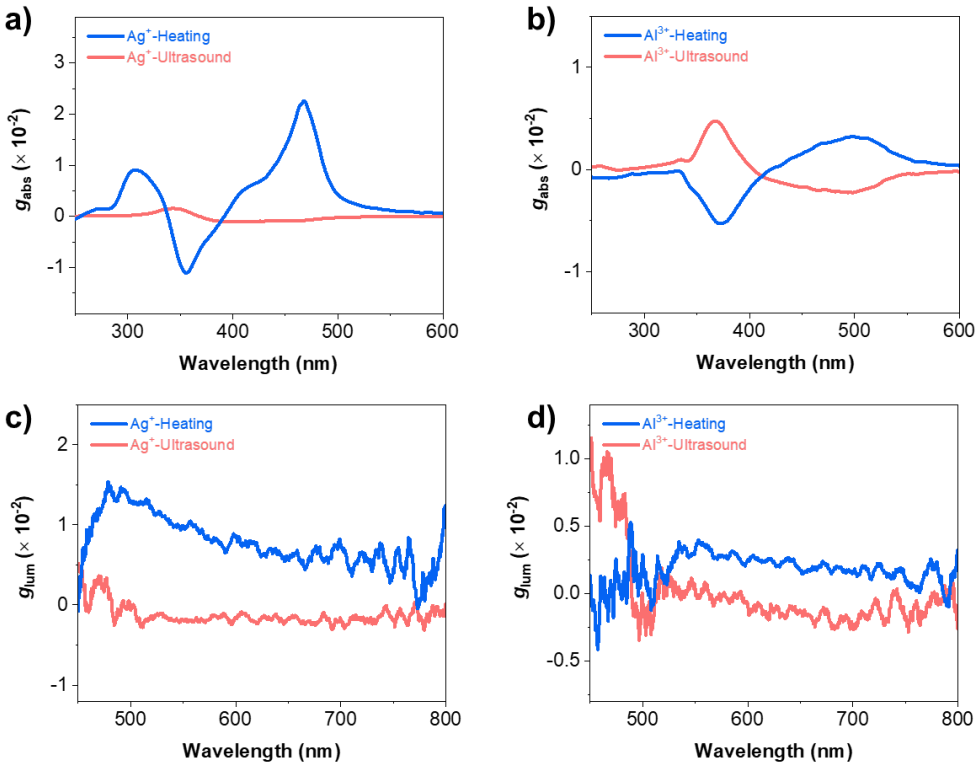

Figure S17. a,b) g_{abs} and c,d) g_{lum} value of a,c) Ag^{+} and b,d) Al^{3+}-based MOSPs in *n*-BuOH after being treated by ultrasound and heating-cooling cycle ([PCSPCC] = 14 mM, $n_{M}{}^{n+}/n_{PCSPCC}$ = 1/2).

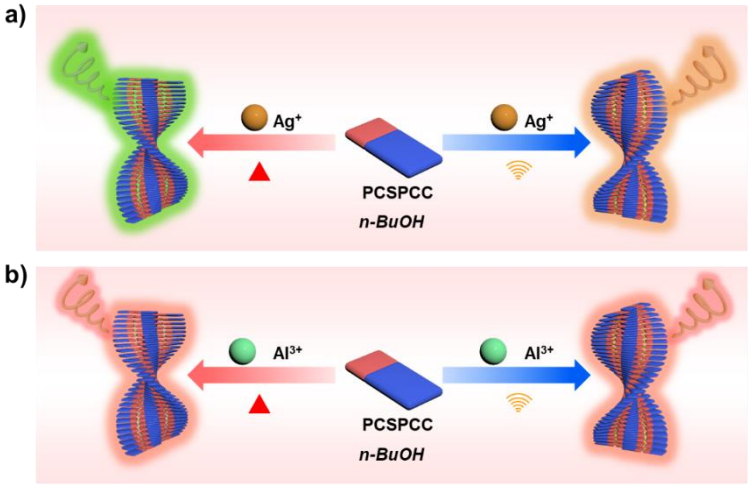

Figure S18. Proposed schematic illustration of CD and CPL inversion of a) PCSPCC+$AgNO_3$ and b) PCSPCC+$AlCl_3$ aggregates treated by heating-cooling cycle and ultrasound in *n*-BuOH.

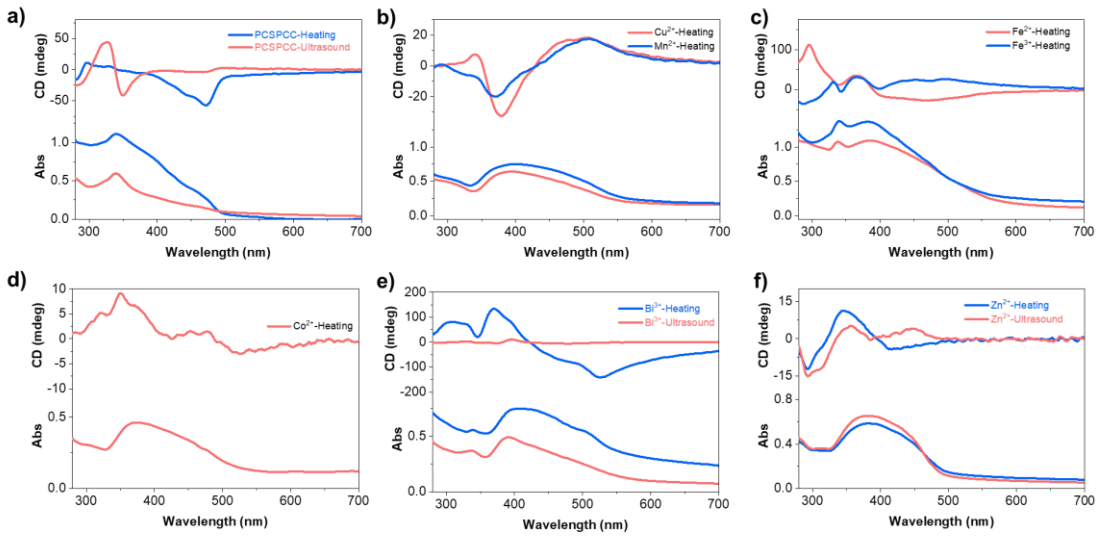

Figure S19. The CD spectra of PCSPCC-based MOSPs treated by heating-cooling cycle and ultrasound in *n*-BuOH, respectively ([PCSPCC] = 14 mM, $n_{M^{n+}}/n_{PCSPCC}$ = 1/2).

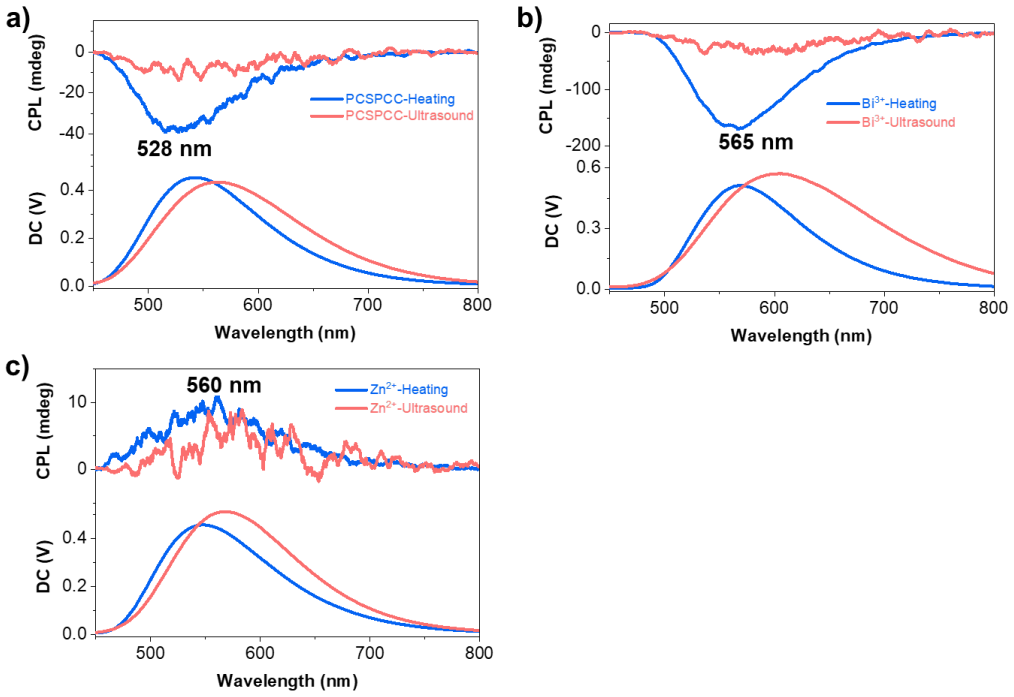

Figure S20. The CPL spectra a) PCSPCC, b) PCSPCC+$BiCl_3$, and c) PCSPCC+$ZnCl_2$ aggregates treated by heating-cooling cycle (blue line) and ultrasound (red line) in *n*-BuOH, respectively ([PCSPCC] = 14 mM, $n_{M^{n+}}/n_{PCSPCC}$ = 1/2).

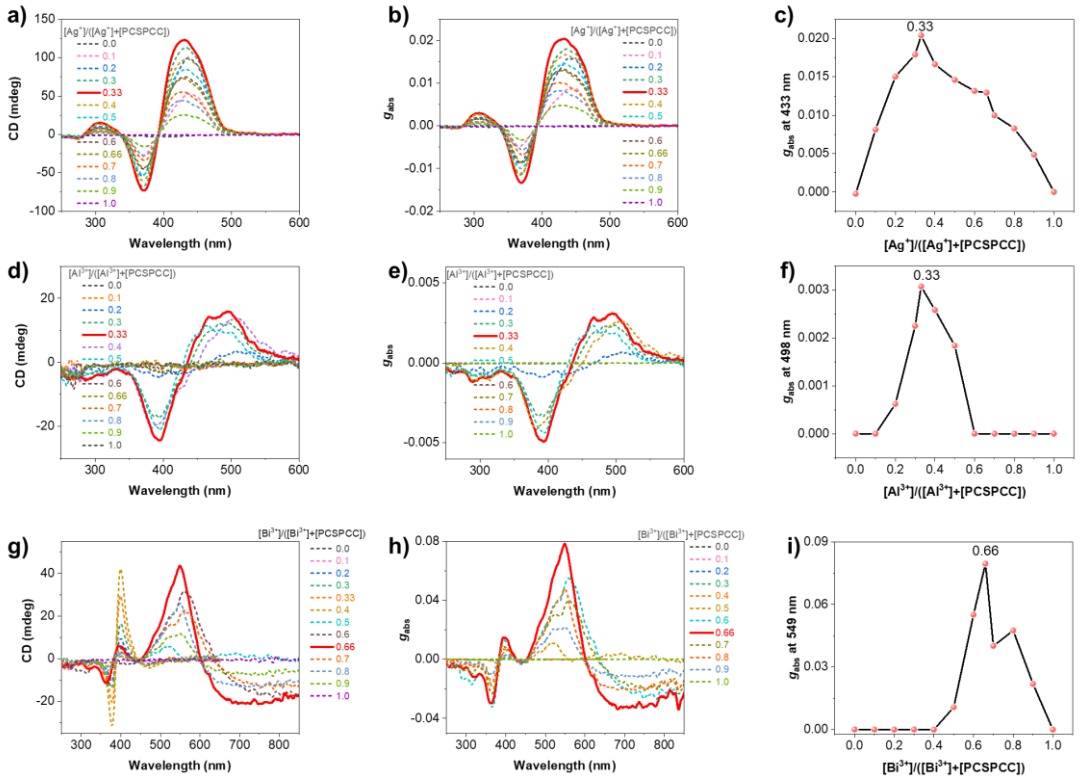

Figure S21. a, d, g) CD measurement, corresponding b, e, h) g_{abs} values and c, f, i) Job's plot curves of PCSPCC-based metal complexes after adding different $[M^{n+}]/([M^{n+}]+[PCSPCC])$ molar ratios of a-c) $AgNO_3$, d-f) $AlCl_3$ and g-i) $BiCl_3$ in PX/*n*-BuOH (*v*/*v*, 1/1).

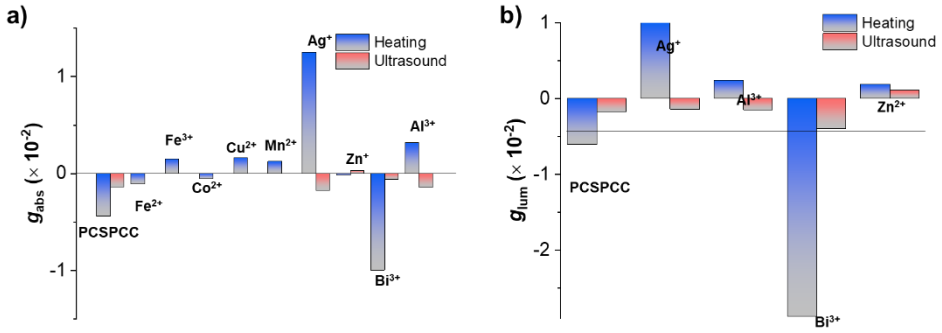

Figure S22. a) g_{abs} and b) g_{lum} value of PCSPCC-based MOSPs in *n*-BuOH.

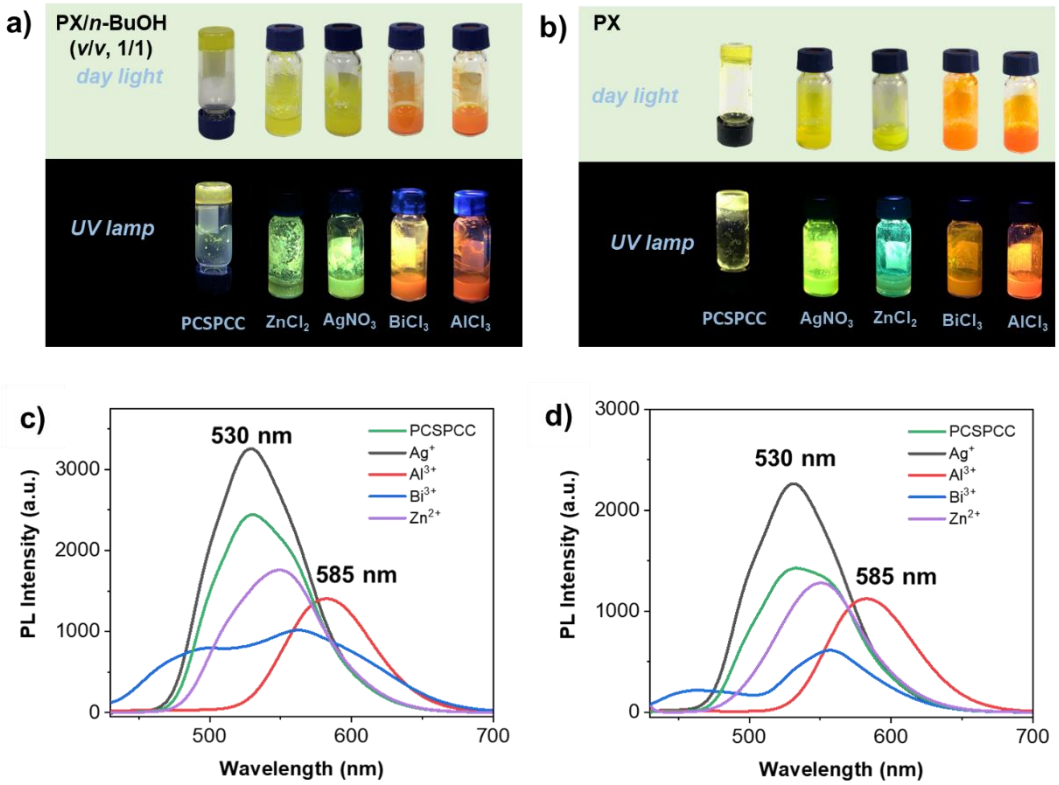

Figure S23. The photographs of PCSPCC-based MOSPs in a) PX/*n*-BuOH (*v*/*v*, 1/1) and b) PX under daylight and UV light irradiation. The PL spectra of PCSPCC co-assembled with various metal ions in c) PX/*n*-BuOH (*v*/*v*, 1/1) and d) PX ([PCSPCC] = 14 mM, $n_{M^{n+}}/n_{PCSPCC}$ = 1/2).

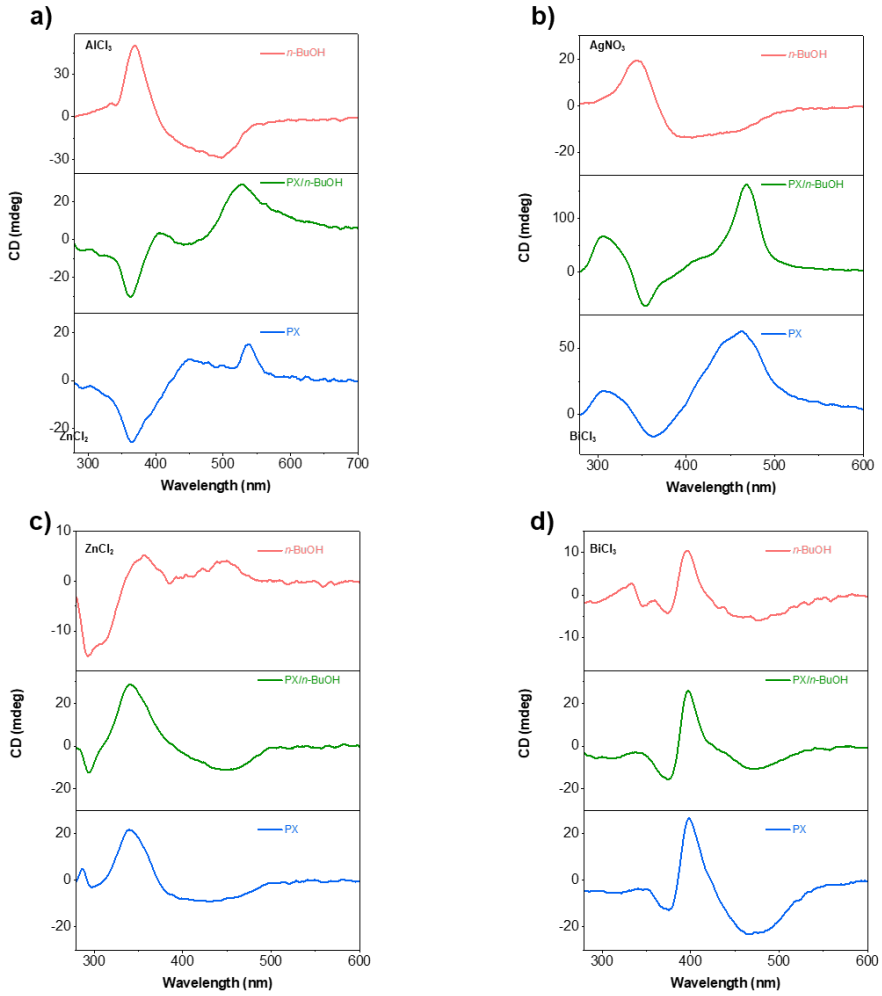

Figure S24. The CD spectra of a) PCSPCC+$AlCl_3$, b) PCSPCC+$AgNO_3$, c) PCSPCC+$ZnCl_2$ and d) PCSPCC+$BiCl_3$ aggregates treated by ultrasound in *n*-BuOH, PX/*n*-BuOH (*v*/*v*, 1/1) and PX, respectively ([PCSPCC] = 14 mM, $n_{M^{n+}}/n_{PCSPCC}$ = 1/2).

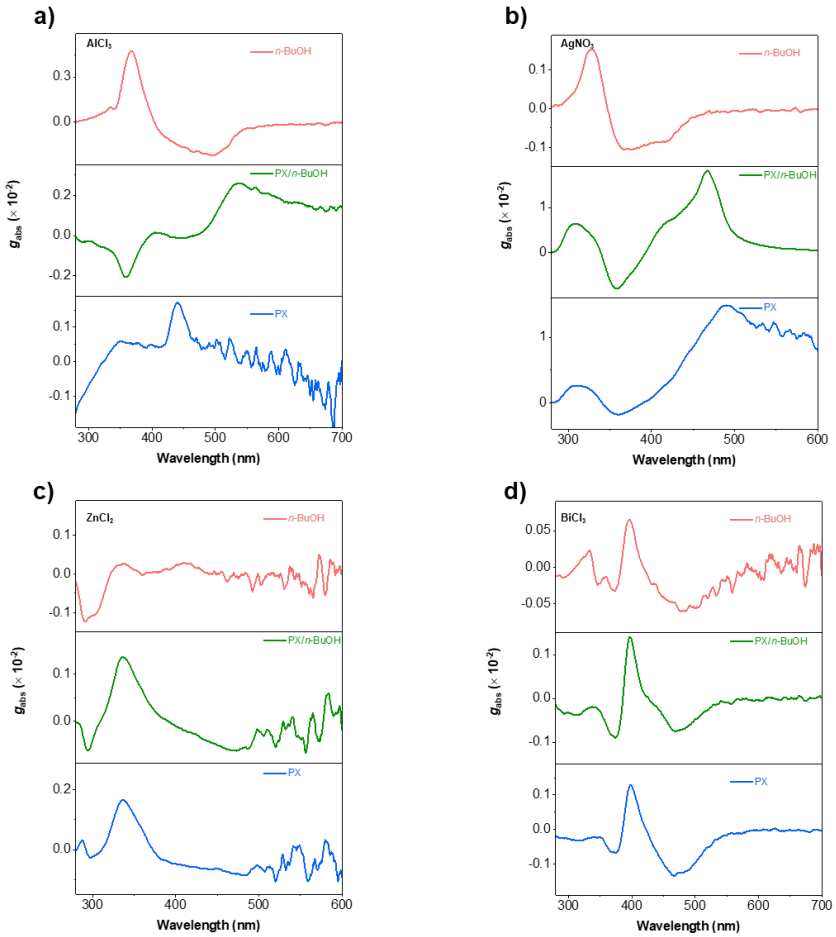

Figure S25. The g_{abs} value of a) PCSPCC+$AlCl_3$, b) PCSPCC+$AgNO_3$, c) PCSPCC+$ZnCl_2$ and d) PCSPCC+$BiCl_3$ aggregates treated by ultrasound in *n*-BuOH, PX/*n*-BuOH (*v*/*v*, 1/1) and PX, respectively ([PCSPCC] = 14 mM, $n_{M^{n+}}/n_{PCSPCC}$ = 1/2).

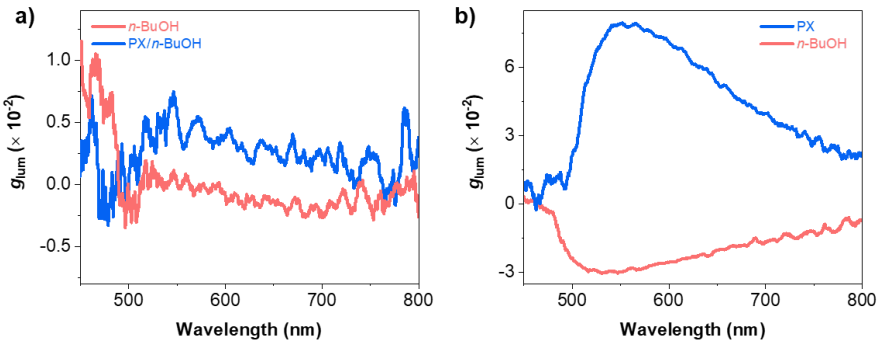

Figure S26. The g_{lum} value of a) PCSPCC+$AlCl_3$ and b) PCSPCC+$BiCl_3$ aggregates treated by a) ultrasound and b) thermal in *n*-BuOH, PX/*n*-BuOH (*v*/*v*, 1/1) and PX, respectively ([PCSPCC] = 14 mM, $n_{M^{n+}}/n_{PCSPCC}$ = 1/2).

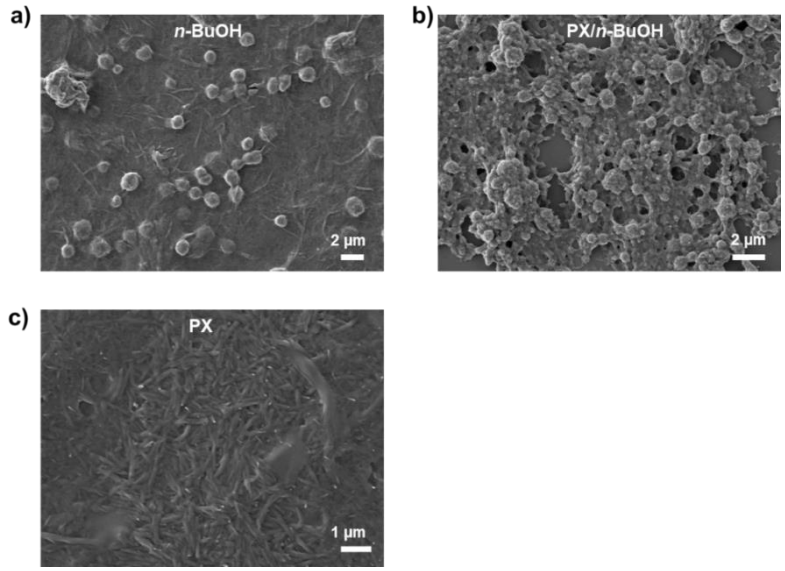

Figure S27. SEM images of PCSPCC+$AlCl_3$ aggregates treated by ultrasound in a) *n*-BuOH, b) PX/*n*-BuOH (*v*/*v*, 1/1), and c) PX.

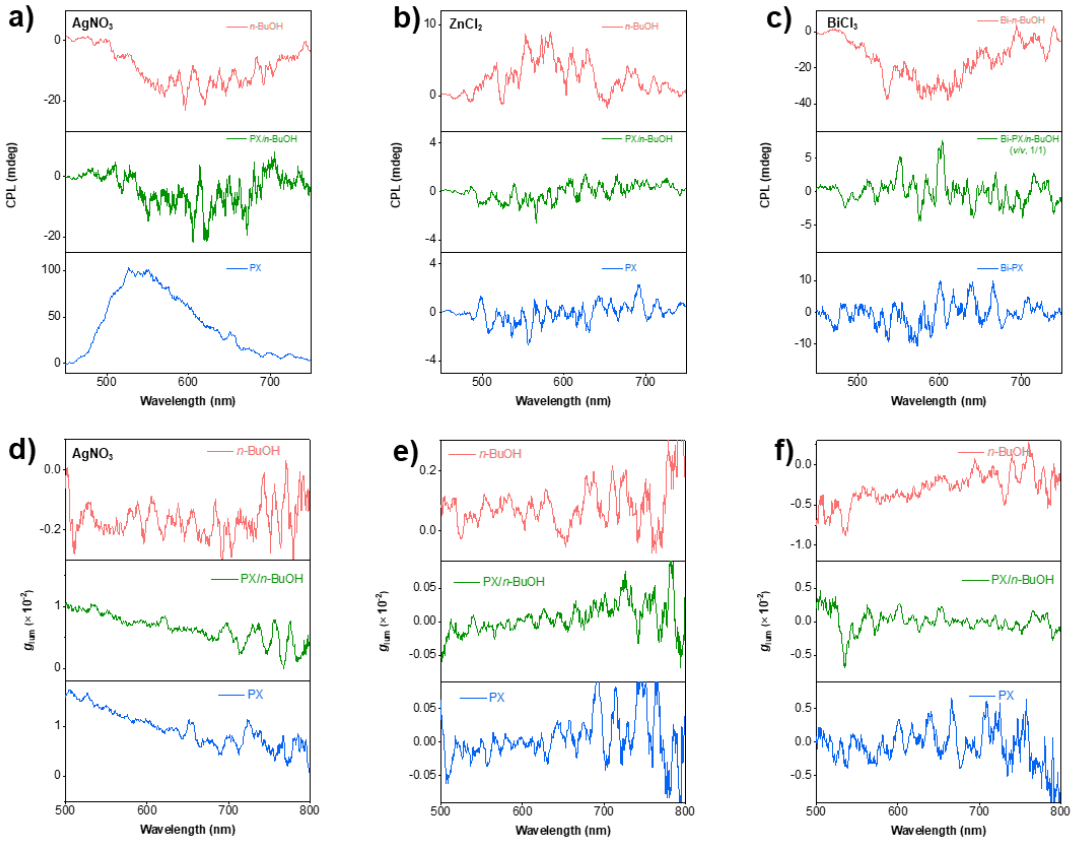

Figure S28. The a-c) CPL spectra and corresponding d-f) g_{lum} value of a,d) PCSPCC+$AgNO_3$, b,e) PCSPCC+$ZnCl_2$, and c,f) PCSPCC+$BiCl_3$ aggregates treated by ultrasound in *n*-BuOH, PX/*n*-BuOH (*v*/*v*, 1/1) and PX, respectively ([PCSPCC] = 14 mM, $n_M{}^{n+}/n_{PCSPCC}$ = 1/2).

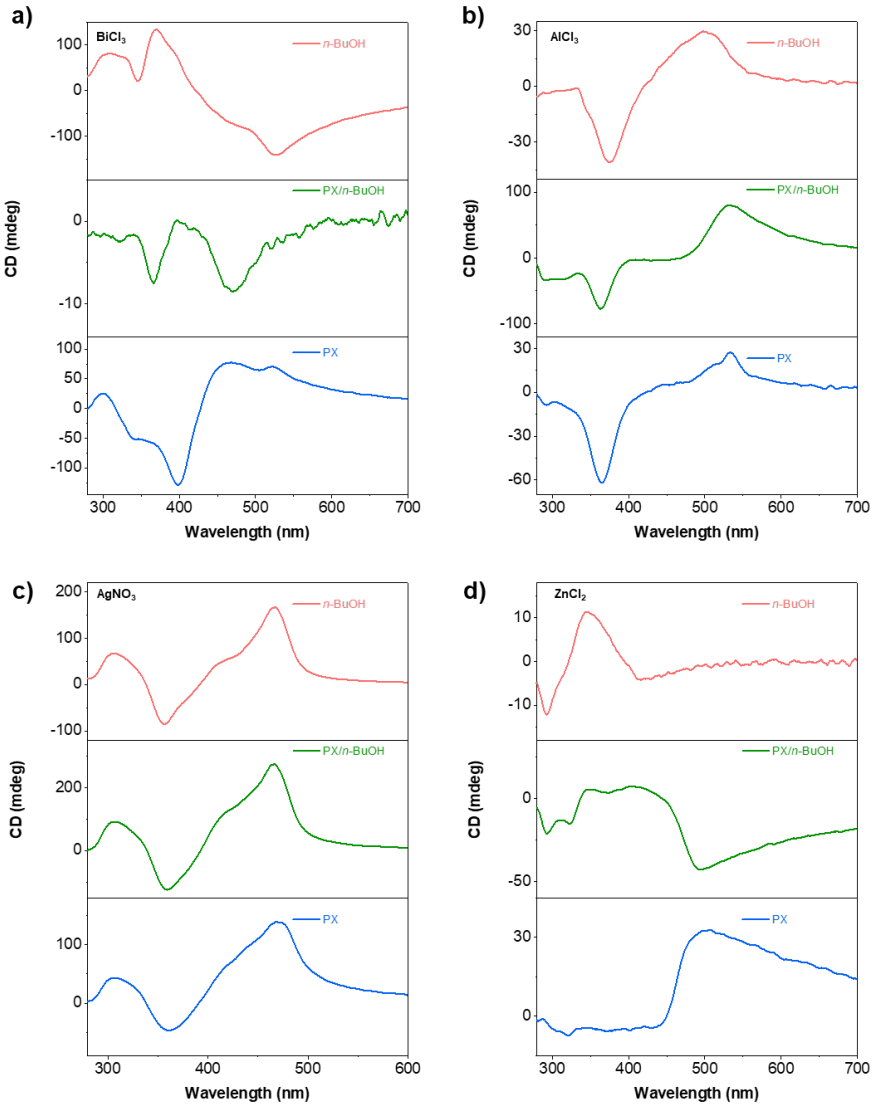

Figure S29. The CD spectra of a) PCSPCC+$BiCl_3$, b) PCSPCC+$AlCl_3$, c) PCSPCC+$AgNO_3$, and d) PCSPCC+$ZnCl_2$ aggregates treated by heating-cooling cycle in *n*-BuOH, PX/*n*-BuOH (*v*/*v*, 1/1) and PX, respectively ([PCSPCC] = 14 mM, $n_{M^{n+}}/n_{PCSPCC}$ = 1/2).

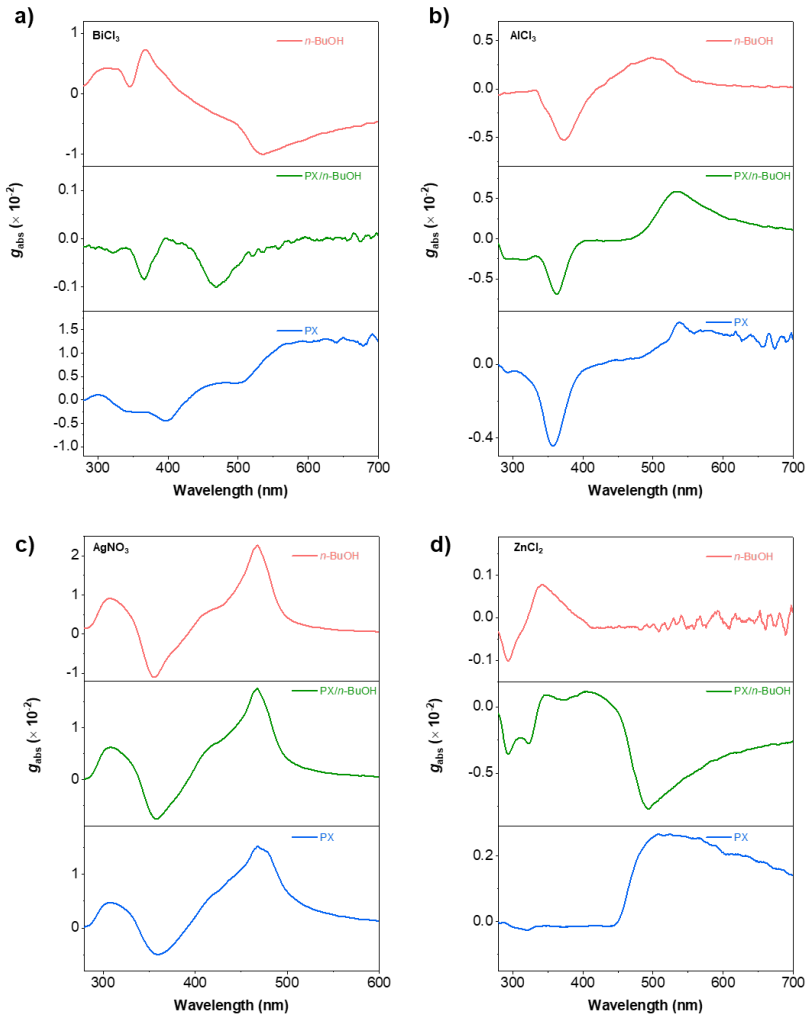

Figure S30. The g_{abs} value of a) PCSPCC+$BiCl_3$, b) PCSPCC+$AlCl_3$, c) PCSPCC+$AgNO_3$, and d) PCSPCC+$ZnCl_2$ aggregates treated by heating-cooling cycle in *n*-BuOH, PX/*n*-BuOH (*v*/*v*, 1/1) and PX, respectively ([PCSPCC] = 14 mM, $n_{M^{n+}}/n_{PCSPCC}$ = 1/2).

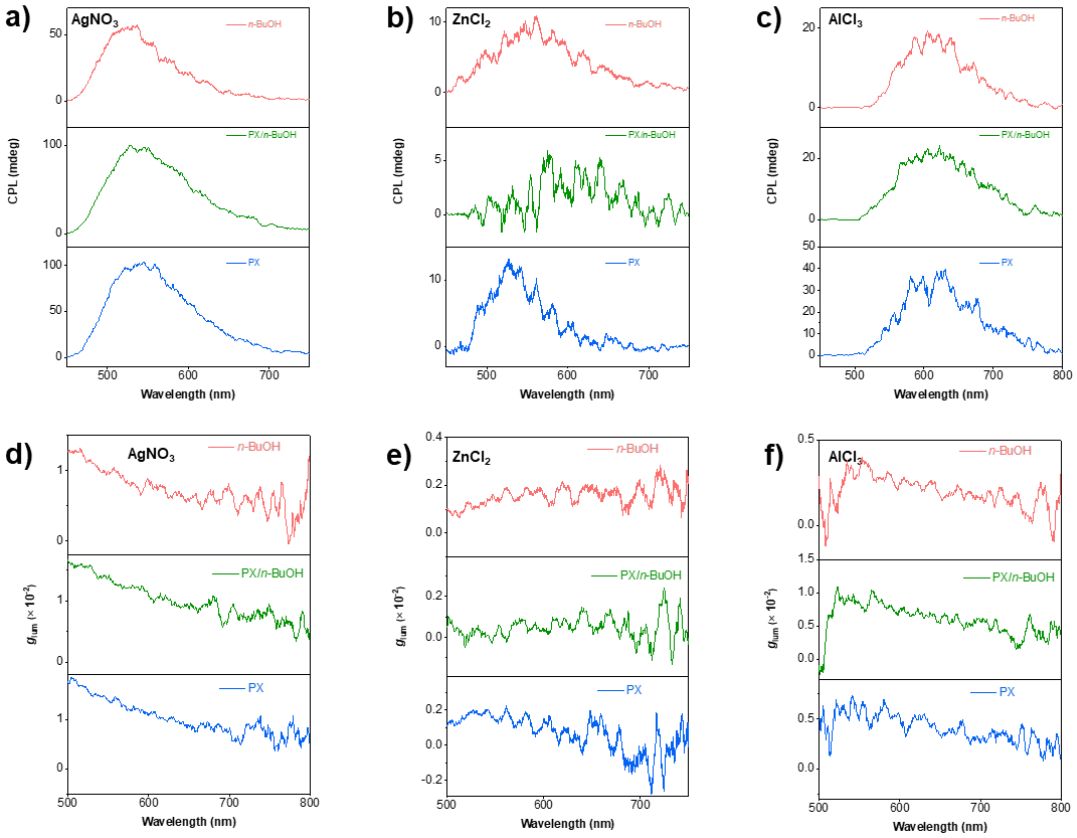

Figure S31. a-c) CPL spectra and d-f) corresponding g_{lum} value of a,d) PCSPCC+$AgNO_3$, b,e) PCSPCC+$ZnCl_2$, c,f) PCSPCC+$BiCl_3$ aggregates treated by the heating-cooling cycle in *n*-BuOH, PX/*n*-BuOH (*v*/*v*, 1/1) and PX, respectively ([PCSPCC] = 14 mM, $n_M{}^{n+}/n_{PCSPCC}$ = 1/2).

Table S1 Data of Ag^+/PCSPCC mixture used for job's plot.

PCSPCC (2×10^{-3} mol)	Ag^+ (2×10^{-3} mol)	$[Ag^+]/([Ag^+]+[PCSPCC])$	g_{abs} at 433 nm
1.0 eq	0 eq	0	-0.0002
0.9 eq	0.1 eq	0.1	0.0081
0.8 eq	0.2 eq	0.2	0.0150
0.7 eq	0.3 eq	0.3	0.0179
0.66 eq	0.33 eq	0.33	0.0204
0.6 eq	0.4 eq	0.4	0.0166
0.5 eq	0.5 eq	0.5	0.0146
0.4 eq	0..6eq	0.6	0.0132
0.33 eq	0.67 eq	0.66	0.0129

0.3 eq	0.7 eq	0.7	0.0010
0.2 eq	0.8 eq	0.8	0.0083
0.1 eq	0.9 eq	0.9	0.0049
0 eq	1.0eq	1.0	0

Table S2 Data of Al^{3+}/PCSPCC mixture used for job's plot.

PCSPCC (2×10^{-3} mol)	Al^{3+} (2×10^{-3} mol)	$[Al^{3+}]/([Al^{3+}]+[PCSPCC])$	g_{abs} at 498 nm
1.0 eq	0 eq	0	0
0.9 eq	0.1 eq	0.1	0
0.8 eq	0.2 eq	0.2	0.0006
0.7 eq	0.3 eq	0.3	0.0023
0.66 eq	0.33 eq	0.33	0.0031
0.6 eq	0.4 eq	0.4	0.0026
0.5 eq	0.5 eq	0.5	0.0018
0.4 eq	0..6eq	0.6	0
0.3 eq	0.7 eq	0.7	0
0.2 eq	0.8 eq	0.8	0
0.1 eq	0.9 eq	0.9	0
0 eq	1.0eq	1.0	0

Table S3 Data of Bi^{3+}/PCSPCC mixture used for job's plot.

PCSPCC (2×10^{-3} mol)	Bi^{3+} (2×10^{-3} mol)	$[Bi^{3+}]/([Bi^{3+}]+[PCSPCC])$	g_{abs} at 549 nm
1.0 eq	0 eq	0	0
0.9 eq	0.1 eq	0.1	0
0.8 eq	0.2 eq	0.2	0
0.7 eq	0.3 eq	0.3	0
0.6 eq	0.4 eq	0.4	0

0.5 eq	0.5 eq	0.5	0.0107
0.4 eq	0.6eq	0.6	0.0551
0.33 eq	0.67 eq	0.66	0.0795
0.3 eq	0.7 eq	0.7	0.0401
0.2 eq	0.8 eq	0.8	0.0475
0.1 eq	0.9 eq	0.9	0.022
0 eq	1.0 eq	1.0	0

Table S4. CPL activity of PCSPCC-based aggregates regulated by treatment modes, metal ions, and solvent effects. "+" represents left-handed CPL, "–" represents right-handed CPL, and "N" stands for the negligible CPL activity.

		PCSPCC	Ag^{+}	Zn^{2+}	Al^{3+}	Bi^{3+}
n-BuOH	Ultrasound	-	-	+	-	-
	Heating	-	+	+	+	-
PX/*n*-BuOH	Ultrasound	-	+	N	+	N
	Heating	-	+	+	+	-
PX	Ultrasound	-	+	N	+	N
	Heating	-	+	+	+	+

3 References

1. Kurzajewska, M.; Kwiatek, D.; Kubicki, M.; Brzezinski, B.; Hnatejko, Z., *Polyhedron* **2018,** *148*, 1-8.
2. Marjani, K.; Mousavi, M.; Hughes, D. L., *Transition Met Chem* **2009,** *34*, 85-89.
3. Liu, G.; Sheng, J.; Teo, W. L.; Yang, G.; Wu, H.; Li, Y.; Zhao, Y.,. *J. Am. Chem. Soc.,* **2018,** *140*, 16275-16283.
4. Wang, Y.; Liu, C.; Fu, K.; Liang, J.; Pang, S.; Liu, G., *Chem. Commun.* **2022,** *58* 9520-9523.